

## Development And Evaluation Of Apremilast-Loaded Nanosponges For Enhanced Wound Healing: A Novel Topical Drug Delivery System

Purnima Rai<sup>\*1</sup>, Dr. A.K.S Rawat<sup>2</sup>

<sup>\*1</sup>Department of Pharmacy, Maharishi University of Information Technology- 226013

Email ID: [purnima93rai@gmail.com](mailto:purnima93rai@gmail.com)

<sup>2</sup>A Ethno-medicine Research Centre Hengbung, Manipur

Email ID: [rawataks@rediffmail.com](mailto:rawataks@rediffmail.com)

Presenting author e-mail: [purnima93rai@gmail.com](mailto:purnima93rai@gmail.com)

### \*Presenting Author:

Purnima Rai

Department of Pharmacy, Maharishi University of Information Technology- 226013

Email ID: [purnima93rai@gmail.com](mailto:purnima93rai@gmail.com)

*Cite this paper as:* Purnima Rai, Dr. A.K.S Rawat, (2025) Development And Evaluation Of Apremilast-Loaded Nanosponges For Enhanced Wound Healing: A Novel Topical Drug Delivery System. *Journal of Neonatal Surgery*, 14 (15s), 1205-1217.

### ABSTRACT

Topical drug delivery technologies are useful for targeted treatment, and nanosponges, with porous designs that can improve drug stability, bioavailability, and controlled release, are becoming increasingly feasible possibilities. The main goal of this research is to create and assess topical nanosponges that contain apremilast to improve wound healing. The PDE4 inhibitor apremilast, which is used to treat inflammatory illness, was introduced to nano-sponges using the emulsion solvent diffusion technique. To minimize particle size, enhance drug release, and optimize encapsulation efficiency, the formulation was optimized using a two-factor, three level experimental approach. Fourier transform infrared spectroscopy (FTIR), X-ray diffraction (XRD), differential scanning calorimetry (DSC), and scanning electron microscopy (SEM) were used to examine the nano-sponges. Based on its high degree of crystallinity, structural integrity, and melting point (154- 157°C), Apremilast's physicochemical stability was confirmed by the results. SEM showed uniform, spherical nanosponges with a porous surface that are ideal for controlled release. A 24-hour controlled drug release of 95.85%, an entrapment efficiency of 82.75%, and a particle size of 213.85 nm were all demonstrated by the improved formulation. The intriguing results of this study addressing Apremilast- loaded nano-sponges as a new wound healing therapy warrant additional clinical investigation. These nano-sponges provide longer therapeutic effect, better medication stability, and more patient compliance.

**Keywords:** Wound healing, Apremilast, Nanosponges, Controlled drug release, Encapsulation efficiency, Topical drug delivery

### 1. INTRODUCTION

Any harm to the integrity of live tissue may be called a wound. The skin, the largest organ in the human body, acts as a barrier between the dry outside air and the body's water-rich internal organs [1].

To be healthy, one must be able to heal wounds can be a significant challenge and burden for healthcare systems. According to Medicare, the expenses for treating acute and chronic wounds are expected to range from \$28.1 billion to \$96.8 billion in 2014 [2].

Wound healing is a set of consecutive occurrences. Initially, bleeding and clotting ensue, followed, by the activation of acute inflammatory response to repair the original injury. Extracellular matrix proteins are then generated, and the new parenchyma and connective tissue are remodeled. In this process, both connective tissues undergo remodeling, migration, and regeneration. This process involves remodeling migration, regeneration, and proliferation. Both connective tissue and parenchymal cells proliferate, migrate, and regenerate during this process.

Deposition of collagen is another crucial element. Lastly, parenchymal cells and these. Deposition of collagen is another crucial element. Ultimately, these coordinated stages lead to the healing of damaged tissues, which fortifies a wound in a systematic way [3].

Topical drug delivery is the technique of putting a medication-containing pharmaceutical formulation directly to the skin to treat a wide range of cutaneous problems, including acne. It can be both therapeutic and inspiring for the patient. Targeted drug distribution to specific skin patches affected by localised ailments has proven to be an effective method. The skin is the primary organ to receive medication via the delivery of topical drugs since it is the most accessible organ for treating topical illnesses. The application of medicinal drugs topically is common to prevent a number of illnesses or ailments. These products include semi-solid formulations utilized in topical drug delivery systems, such as ointments, creams, powders, sprays, gels, and medicated adhesive systems [4].

Materials that resemble sponges and have tiny holes with an average diameter of less than 1µm are called nano-sponges [5]. A sponge can be a long polyester strip dissolved in a fluid containing crosslinkers, which act as microscopic hooking snares to hold various polymer components together. Nano-sponge are similar to three-dimensional structures [6]. This tiny sponge may circulate throughout the body until it reaches a certain location, adheres to the skin, and, in some situations, starts to release medication. Due to its ability to be released at a specific target location as opposed to circulating throughout the body, the drug will work better for a given dosage. Within their network, NS may bind less soluble medication increasing their bioavailability.

They are also very good at entrapping a wide range of excipients [7]. The FDA has authorised a novel drug called apremilast, which inhibits phosphodiesterase 4 enzymes and increases c-AMP levels. Tumor necrosis factor alpha (TNF) production by human rheumatoid synovial cells is spontaneously suppressed as a result of phosphodiesterase-4 inhibition. The nanosponge developed by Apremilast offers better bioavailability, less dosing frequency, and increased pharmaceutical stability. Topical amphotericin B nanosponge gel penetrates the skin and helps to give a higher therapeutic dose of medication through the epidermis [8,9].

The advantages of utilizing experimental design to optimize nanoparticles include fewer experiments, the construction of mathematical models to estimate the statistical significance & importance of factor effects, and the assessment of component interaction effects [10]. A two-factor, three-level experimental strategy was used to optimize the NS synthesis procedure.

## 2. MATERIAL AND METHODS

### Material

The materials listed below were obtained from the specified sources without further purification. Apremilast was obtained from INSCHM, which is based in Lucknow, Uttar Pradesh, India. The remaining chemicals utilized were analytical reagent grade.

### Methods

#### Pre-formulation research

##### Determining the melting point

The melting point of Apremilast was established with a melting point equipment. A glass capillary with one end sealed with flame was filled with aprimilast. A liquid paraffin bath was used within the melting point apparatus to submerge the capillary containing Apremilast.

The liquid paraffin was heated until Apremilast melted. Apremilast's melting temperature was recorded [11].

##### Solubility Study

Apremilast's solubility in various solvents was evaluated using the shake flask method to fulfil regulatory criteria. Apremilast's solubility was tested in various solvents, including ethanol, water, isopropyl myristate, and octanol.

##### UV visible Spectroscopy

##### Standard Preparation

To prepare a standard stock solution of 100 µg/ml, Apremilast was dissolved in ethanol. Diluting the stock solution yielded concentrations ranging from 1 to 6 µg/ml.

##### Determination of wavelength

The electrical structure of the compound or analyte that contributes compound property. The spectral analysis was performed using an Apremilast reference solution in the UV range of 200-400 nm.

##### 2.2.1.2. FT-IR, or Fourier Transform Infra-Red Spectroscopy

For the identification of both organic and inorganic molecules, the FT-IR approach is very helpful. This device can be used to measure certain components of an unknown mixture and to evaluate solids, liquids, and gases [12]. Flucytosine was measured using Fourier Transform Infra-Red Spectroscopy (FT-IR) with the Perkin Elmer Spectrum IR version.

10.7.2. The spectra were generated by the KBr pellet technique, and the reference standard peaks were compared to the obtained ones. 10 mg of Apremilast was mixed with KBr under high compaction pressure. The spectra of the dry drug-polymer mixture were obtained after baseline correction and recorded using scanning.

### 2.2.1.3 Drug - excipients compatibility studies

Any chemical or physical interaction between medications and excipients has the potential to impact drug stability and bioavailability. We prepared a modest mixture of medicines and excipients in a 1:1 ratio. The mixtures were placed in the vials shown above. The rubber closures were placed on the vials, sealing them hermetically. The drug-excipient compatibility was assessed after four weeks of storage at ambient temperatures. The samples were also analyzed using the FTIR technique [13].

### 2.2.1.4 X-ray diffraction (XRD) study

X-ray diffraction (XRD) is a highly effective and widely used tool in research and industry. Although XRD is well known for its capacity to qualitatively and quantitatively analyze crystalline phases in materials, a thorough inspection of the diffraction patterns can reveal a plethora of other information. An XRD study was performed on the pure medicine in order to quantify, diffraction pattern [14].

### Differential scanning calorimetry (DSC)

The thermal behaviour of pure medicines in combination and individually was investigated using DSC Mettler (Perkin Elmer). In sealed aluminum pans, the samples were heated between 500 and 3000 degrees Celsius at a rate of 500 degrees per minute. The rate at which nitrogen gas is purged is 30 milliliters per minute. A reference was an empty aluminum pan [15].

## 3. FORMULATION DEVELOPMENT

### Preparation of Nano-emulsion as per the Experimental Design

To demonstrate the response surface model, a set of values was obtained using Design Expert® (Version 12.0.3.0) software. A two-factor, three-level experimental strategy was used to optimize the NS synthesis procedure. Design Expert® (Version 12.0.3.0) was used to explore the response surfaces, which were represented by an optimization process with a small number of experimental runs (in the current study, 09 runs). The concentration of EC:PVC ratio (X1) and sonication time (X2), with their respective set low (−1), medium (0), and high (+1) levels, were the independent factors chosen based on preliminary studies. Particle size (Y1), entrapment efficiency (%) (Y2), and drug release percentage (Y3) were the dependent responses that were examined. Two components and only nine runs are required, resulting in decreased time and energy consumption. Furthermore, each element is investigated and classified at three fundamental levels. Table 1 shows an outline of the implied dependent and independent variables [16].

**Table 1: Central Composite Design Variables.**

Factor independent variable	Levels applied		
	-1	0	+1
Concentration of EC: PVA Ratio (%) (X1)	1	3	5
Time of Sonication (X2)	10	15	20
Dependent variables	Constraints		
Size of Particles (nm) (Y1)	Minimize		
% Entrapment Efficiency (%) (Y2)	Maximize		
% Drug Release (%) (Y3)	Maximize		

**Table 2: Box-Behnken design's composition and observed responses**

Batch	Drug (mg)	Independent Factors		Dependent Factors		
		Concentration of EC:PVA ratio (%)	Sonication Duration (Min)	Size of particle (nm)	% Entrapment efficiency	% Drug Release
NS1	20	5.82843	15	197.13	63.24	76.83
NS2	20	1	10	202.6	60.22	79.81
NS3	20	5	20	207.5	69.82	74.94
NS4	20	1	20	229.21	60.23	91.93
NS5	20	3	7.92893	216.13	70.91	93.41
NS6	20	0.171573	15	211.34	61.95	82.56
NS7	20	3	22.0711	237.42	73.22	81.56
NS8	20	3	15	213.85	82.75	95.85
NS9	20	5	10	208.57	65.82	88.71

#### Formulation by Emulsion Solvent Diffusion Method

The nano-sponges were created by dissolving the prescribed amounts of polymers, in the right drug ratios, in 20 millilitres of dichloromethane (DCM). Apremilast was then added to the solution, which was agitated with a magnetic stirrer until completely dissolved. It was proposed that this was an interior phase of organic matter. After that, the aqueous external phase—which contained the appropriate quantity of PVA dissolved in 100 milliliters of distilled water—was gradually supplemented with the organic internal phase. The mixture was agitated for two hours at 800-1000 rpm using a magnetic stirrer. The resulting dispersion was filtered and dried for 24 hours at 40°C. The powder that was produced was used for characterization.

#### 4. EVALUATION OF NANO-SPONGES

##### Percentage encapsulation efficiency

When evaluating the efficacy of a medication delivery strategy, encapsulation efficiency is a crucial factor. This technique entails forming a shell around a medicine to keep it from leaching out before reaching its target. Encapsulation efficiency is the percentage of the drug that is successfully trapped within the nano-sponges, indicating how much medicine is efficiently supplied in comparison to how much is encapsulated. The drug was loaded. Nano-sponges were centrifuged at 13000 rpm for 40 minutes, and the supernatant liquid was tested for non-bound medication using a UV spectrophotometer at 250 nm. Then the percentage encapsulation efficiency was calculated.

##### In-vitro Drug release

An in-vitro drug release study is an important metric for determining product safety and efficacy since it provides critical information on dosage form behaviour. By revealing crucial details on the dose form, behavior, release mechanism, & kinetics, in-vitro release profiles provide a more logical and scientific approach to drug development. These investigations were carried out on NS formulations utilizing a release cell that resembled a Franz diffusion cell. In short, a wetted cellophane membrane was stretched over the open end of a glass tube. Water tightness was achieved by using a rubber band. 100 mg of NS was inserted in the donor compartment (glass tube above the cellophane membrane). The drug content was measured at 250 nm using a UV spectrophotometer. PBS of 50ml (pH 7.1) was put in a 100ml beaker that was thermostatically regulated (50 rpm) at 37°C (i.e., receptor compartment), and the glass tube was plunged vertically. 5 ml samples of the release media were collected from the area containing receptors at predefined time intervals up to 24 h, while sink conditions were maintained.

##### Particle size and particle size distribution (PDI)

Size of the nano-emulsion particles was measured three times with the ZetasizerVer 7.13 (Malvern Instruments, Ltd, UK). An aliquot of approximately one millilitre was extracted and transferred to a cuvette. The mean particle diameter and polydispersity index (PDI) were measured at 25±2°C with a light scattering angle of 90°. Polydispersity index (PDI) was

utilized to determine the dispersion and homogeneity of the globules.

### Zeta Potential

Surface charge can be measured by the zeta potential. An instrument called a Zeta Sizer (Malvern Instruments) can measure the surface charge (electrophoretic mobility) of a nanosponge using zeta cells, polycarbonate cells with gold-plated electrodes, and water as the sample medium. It is critical for characterizing the stability of nanosponges.

### Particle Morphology

Scanning electron microscopy (SEM) is used to examine nanosponges' surface morphology.

## 5. RESULTS AND CONVERSATIONS

### Pre-formulation research:

#### Melting point determination:

Melting point of apremilast was found to be 154-157°C.

#### Solubility Study:

According to Table 3, the solubility test for apremilast was conducted in a variety of solvents, including ethanol, methanol, chloroform, acetone, octanol, and water.

**Table 3: Solubility test of Apremilast in different solvents**

Sr.No.	Solvent	Soluble	Sparingly Soluble	Insoluble
1	Ethanol	•	-	-
2	Methanol	•		
3	Chloroform	•		
4	Acetone	•		
5	Octanol	•	-	-
6	Water	-	-	•

### UVvisible Spectroscopy

Absorption maxima ( $\lambda_{max}$ ) of the Apremilast was conducted in ethanol. It was found to be 230 nm, shown in fig. 1.

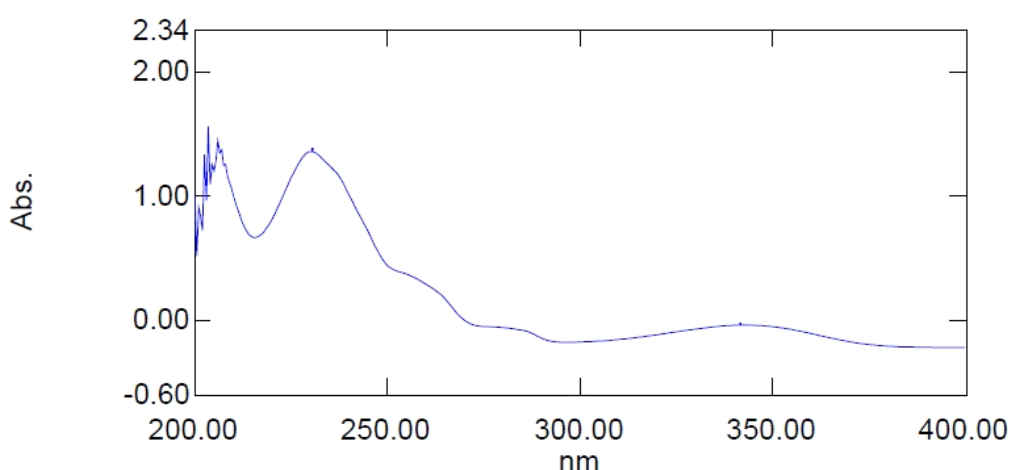


**Fig. 1: UV Spectrum of Apremilast**

The UV-Vis spectrum contains essential information about the compound's electronic transitions and can be utilized for both qualitative and quantitative research. The strong peak at roughly 230 nm is a useful property for identifying or quantifying this component in a mixture or as part of a formulation research.

### Fourier Transform Infra-Red Spectroscopy (FTIR)

Apremilast's molecular structure shows multiple peaks, including O-H stretching vibration ( $3363.58\text{ cm}^{-1}$ ), C-H stretching of aromatic or aliphatic compounds ( $3003.02\text{ cm}^{-1}$ ), and C-H stretching of aldehydes or aliphatic. Figure 2 depicts C-H stretching ( $2837.82\text{ cm}^{-1}$ ), C=O stretching ( $1764.75\text{ cm}^{-1}$ ), C=O stretching ( $1705.14\text{ cm}^{-1}$ ), C=C stretching in aromatic rings ( $1618.23\text{ cm}^{-1}$ ), C-N stretching ( $1348.36\text{ cm}^{-1}$ ), and C-O stretching ( $1022.97\text{ cm}^{-1}$ ).

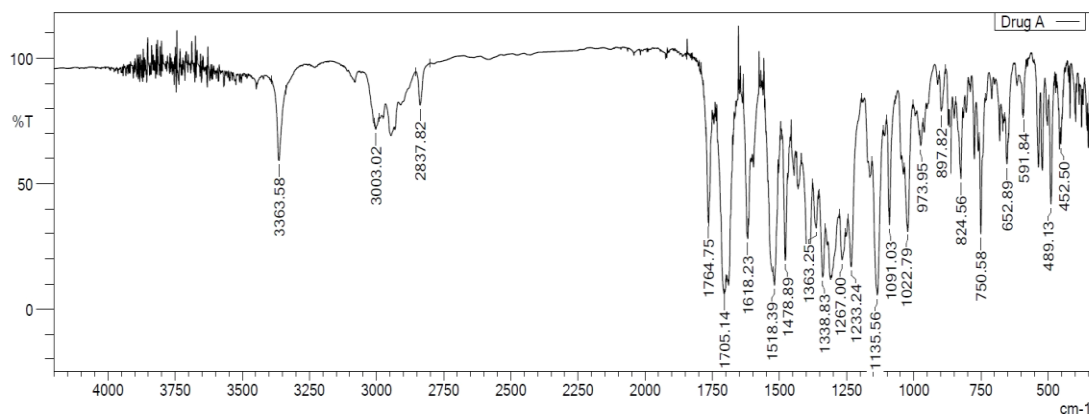


**Fig. 2: FTIR Spectrum of Apremilast**

The FTIR spectrum provides information about the functional groups in the molecule. The significant peaks seen can be linked to certain bonds and functional groups in the Apremilast structure. C=O stretching peaks at  $1764.75\text{ cm}^{-1}$  and  $1705.14\text{ cm}^{-1}$  suggest carbonyl functionalities, such as ester or amide groups. The large peak at  $3363.58\text{ cm}^{-1}$  suggests the existence of hydroxyl or amino groups. Aromatic C-H stretching vibrations at  $3003.02\text{ cm}^{-1}$  confirm the compound's aromatic character. The fingerprint region, with numerous unique peaks, verifies Apremilast's complicated structure, which comprises aromatic rings, carbonyl groups, and potentially ethers or alcohols. This FTIR spectrum confirms Apremilast's identity by comparing it to reference spectra and identifying the characteristic functional groups. The strong and prominent peaks in critical locations indicate that the Apremilast molecule contains the expected chemical capabilities.

### Drug - excipients compatibility studies

Apremilast with excipients exhibits several peaks, such as O-H or N-H stretching vibration ( $4333.95\text{ cm}^{-1}$ ), O-H stretching vibration ( $3364.30\text{ cm}^{-1}$ ), possibly from hydroxyl groups in PVA, C-H stretching of aliphatic chains ( $2888.82\text{ cm}^{-1}$ ), possibly from ethyl cellulose or other hydrocarbon components, C=O stretching vibration ( $1763.31\text{ cm}^{-1}$ ), indicating the presence of carbonyl groups, likely from ester functionalities in ethyl cellulose, C-N stretching in amines or bending vibrations in  $-\text{CH}_3$  groups ( $1364.57\text{ cm}^{-1}$ ), C-O stretching in esters or ethers ( $1262.05\text{ cm}^{-1}$  and  $1234.67\text{ cm}^{-1}$ ) particularly from ethyl cellulose, shown in fig. 3.

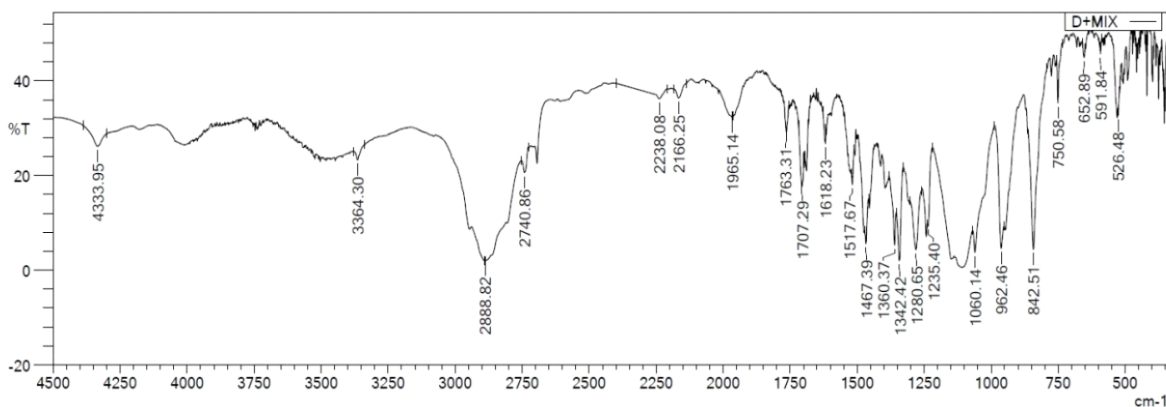


**Fig. 3: FTIR spectrum of drug with excipients**



FTIR spectrum, the mixture containing Apremilast with ethyl cellulose, polyvinyl alcohol, & other excipients show various functional groups' presence, indicating the successful incorporation of these excipients with the active pharmaceutical ingredient (API), Apremilast. Excipients like ethyl cellulose and PVA have characteristic peaks, such as the C=O stretching around  $1763.31\text{ cm}^{-1}$  (from ethyl cellulose) and O-H stretching around  $3364.30\text{ cm}^{-1}$  (likely from PVA or residual moisture). These peaks are superimposed with the peaks of Apremilast, leading to a complex spectrum that reflects the chemical environment of the API within the matrix of excipients. The presence of multiple carbonyl peaks ( $1763.31\text{ cm}^{-1}$  and  $1707.29\text{ cm}^{-1}$ ) suggests that the Apremilast is interacting with the excipients, possibly forming intermolecular hydrogen bonds or other interactions that stabilize the API in the mixture. Lower wavenumber areas ( $1500\text{--}500\text{ cm}^{-1}$ ) have several peaks indicating complicated chemical vibrations of mixed compounds. These include bending and stretching modes of C-H, C-O, and other bonds, which represent the formulation's different chemical environments. The overall spectrum indicates that Apremilast was successfully mixed with the excipients, and there may be some interaction between them, which could affect the drug's stability, release profile, or other physicochemical aspects. This type of analysis is crucial in the development of pharmaceutical formulations, ensuring that the medicine remains stable and effective when coupled with excipients.

#### (XRD) X-ray diffraction analysis:

The XRD analysis of apremilast reveals a crystalline structure with distinct diffraction peaks at  $10^\circ$ ,  $15^\circ$ ,  $20^\circ$ , and  $25^\circ$ , indicating well-organized atomic arrangements. The sharp peak at  $20^\circ$  indicates high crystallinity. The sharp and narrow peaks indicate that the sample is highly crystalline, with little amorphous component. The minimal background noise suggests that the sample is mainly crystalline. A tight match between measured and computed data indicates that the structure is consistent with the theoretical crystal form of apremilast, revealing that the sample is pure, well-crystallized, and constituted of a single crystalline phase devoid of polymorphic forms and impurities (fig. 4).

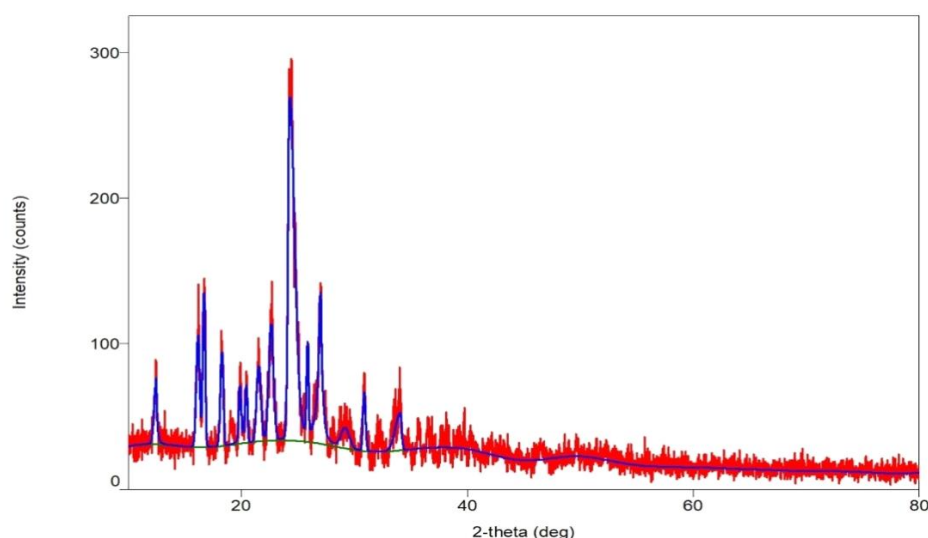


**Fig. 4: XRD of Apremilast**

The XRD analysis of apremilast reveals significant details regarding its crystalline structure, implying that the material is well-organized and pure. Significant peaks at  $10^\circ$ ,  $15^\circ$ ,  $20^\circ$ , and  $25^\circ$  suggest a highly structured atomic arrangement, which is characteristic of a crystalline structure. The steep peak at  $20^\circ$  is a strong indicator of high crystallinity. The absence of significant peaks or anomalies indicates that the sample includes very little amorphous stuff, bolstering its cleanliness. Furthermore, the close match between measured and theoretical data confirms the crystal structure's uniformity, revealing a single crystalline phase without polymorphic variants or contaminants. This demonstrates that the apremilast sample is of high quality, making it suitable for pharmaceutical applications that need crystalline purity.

#### Differential Scanning Calorimetry (DSC)

The Differential Scanning Calorimetry (DSC) graph displays thermal analysis results for a sample designated as Apremilast. The graph's important points include a start temperature of  $157.25^\circ\text{C}$  and a final temperature of  $159.56^\circ\text{C}$ . The sharp endothermic peak on the DSC curve between  $157.25^\circ\text{C}$  and  $159.56^\circ\text{C}$  corresponds to Apremilast's melting point. The onset temperature ( $157.25^\circ\text{C}$ ) signifies the start of melting, while the end temperature ( $159.56^\circ\text{C}$ ) indicates complete melting of the substance. Following the melting event, the graph shows an increase in heat flow, which may imply additional thermal events such as breakdown or phase transitions. The exothermic spike around  $300^\circ\text{C}$  to  $400^\circ\text{C}$  may indicate thermal damage or decomposition of the sample. This is to be expected, as most organic compounds, including medications, disintegrate at higher temperatures. The baseline previous to the melting event ( $30^\circ\text{C}$  to  $157^\circ\text{C}$ ) is reasonably steady, indicating that no

important thermal events (e.g., glass transition or crystallization) occur before the melting point is reached, shown (fig. 5).

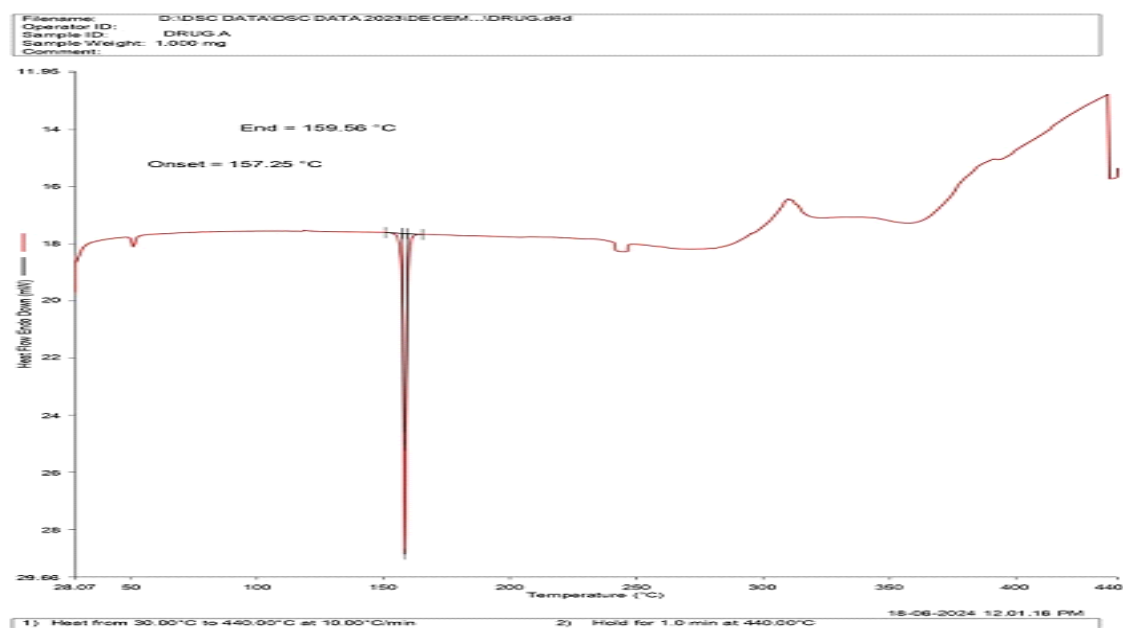


**Fig. 5: DSC of Apremilast**

Apremilast's narrow and well-defined melting range suggests that the sample is highly pure, which is critical for its effectiveness and safety in pharmaceutical applications. Any contaminants in the sample would likely result in a broader melting range or additional peaks on the DSC curve. The data suggest that Apremilast is thermally stable until it reaches its melting point of roughly 157°C. Beyond that, temperature stability would be a key consideration, especially during the manufacturing, storage, and handling processes. The observed thermal deterioration (perhaps indicated by the exothermic rise after melting) shows that Apremilast should not be exposed to high temperatures during processing.

## 6. FORMULATION DEVELOPMENT

### Experimental Design for the Formulation of Nano-sponges

Response surface methodology (RSM), a set of statistical and mathematical approaches, helps in carrying out systematic analysis of formulations. The technique enables the optimization of critical process parameters that can influence the response surface. Using RSM, existing relation between process parameters can be quantified at various levels using the derived response surfaces. Central composite statistical screening design was utilized by using Design Expert® (Version 12.0.3.0) for evaluating main effects, quadratic effects, and the interaction between independent and dependent variables. One of the response surface designs is the central composite design, which offers numerous advantages over other designs. It also includes a multidimensional cube's duplicate center point. Consequently, it only calls for variables to be tested at three levels and stays away from excessive therapy combinations.

Additionally, the projected response's variance at any given position is solely determined by its separation from the design center point. The dependent and independent variables of the applicable CCD have low, medium, and high levels of coded and actual values.

Based on the experimental design, the factor combinations produced 09 different NS formulations batches. As suggested, various NS batches were made and then tested for both reactions.

After fitting the observed answers to 09 runs, it proved that the quadratic model best suited the two dependent variables. the model's importance as well as the terms that are produced and examined. The relationship between the independent and dependent variables, along with all of the responses received for the 09 runs, are shown in Table 2.

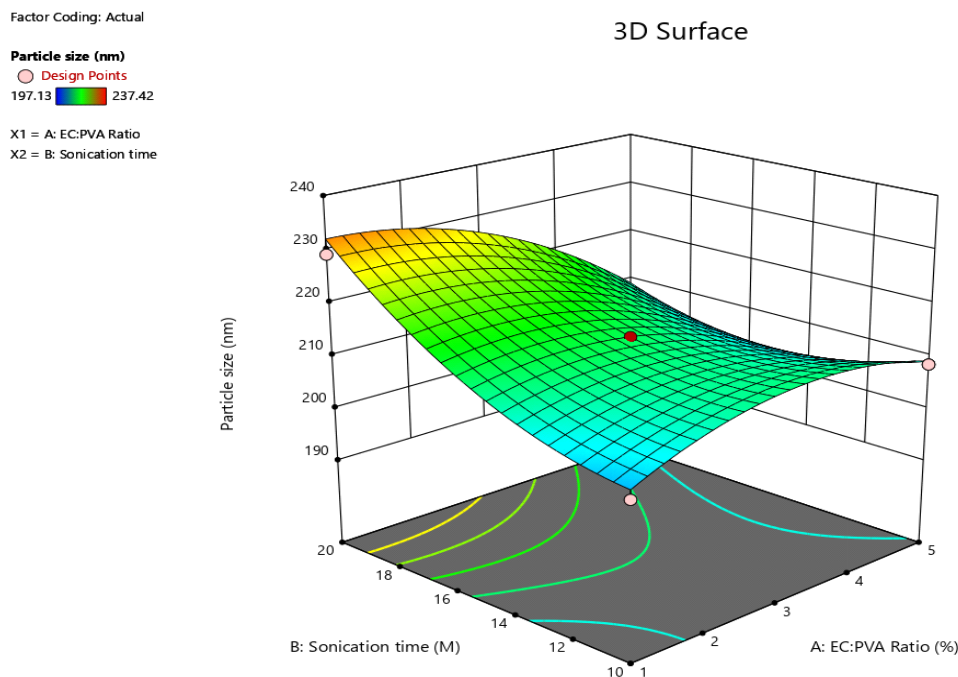
### Effect of independent variables on particle size

Figure 6 shows a 3-D response surface plot demonstrating how the independent variable affects particle size. Because particle size has a significant impact on drug release rate, extent, and

absorption, it is an important factor in the operation of nano-sponges. As particle size reduces, the interfacial area accessible for drug diffusion increases, resulting in improved drug release. The average particle sizes of the created NS formulations



were found to be within the range that suggests consistency in the particle size distribution.



**Fig. 6: Response 3D plots for the effect of EC:PVA ratio (X1) and sonication time (X2) on particle size**

According to the study, when the EC:PVA ratio increases, particle size falls, with greater EC: PVA levels producing smaller nanoparticles. With increased sonication time, the size initially decreases but subsequently stabilizes or slightly increases. Smaller particles result from intermediate sonication times, whereas larger particles result from shorter or longer sonication times. The EC:PVA ratio and sonication time interact to influence particle size. The study suggests that moderate sonication periods and a greater EC:PVA ratio are best for producing the lowest particle sizes. However, extremely long sonication times or low EC:PVA ratios can result in larger particles due to insufficient polymer dispersion or coalescence. Further experimental validation is required to confirm these findings and identify additional parameters influencing particle size.

#### **Independent variables' impact on the percentage of entrapment efficiency**

Figure 7 shows a 3-D response surface plot demonstrating how the independent variable affects the percentage entrapment efficiency. Using the concentration of free medication in the dispersion medium, researchers were able to quantify the entrapment efficiencies of developed formulations. It was clear that as the medication-to-polymer ratio varied, EE altered dramatically. Table 8.14 shows the % entrapment efficiencies for nanosponges. The percentage entrapment effectiveness ranged from 82.25% to 59.62%.

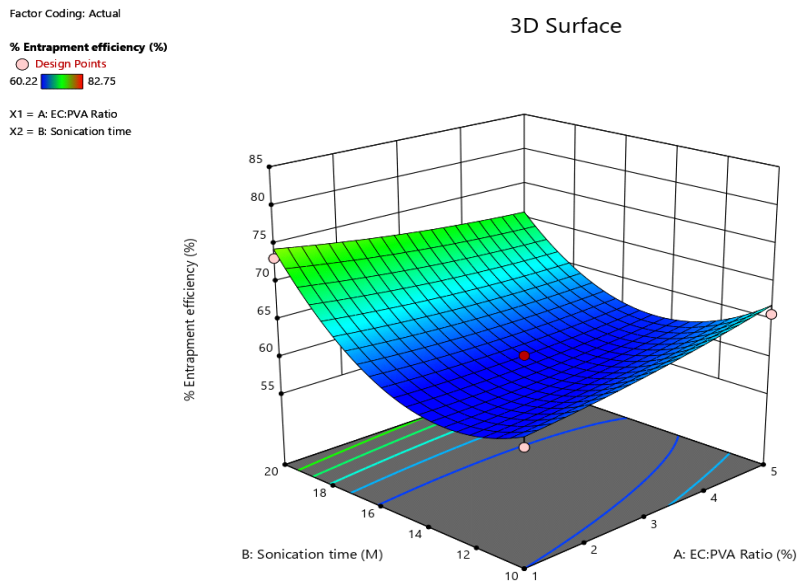


**Fig. 7: Response 3D plots for the effect of EC:PVA ratio (X1) and sonication time (X2) on % Entrapment efficiency**

Entrapment efficiency in nanoparticles is minimal at low EC:PVA ratios; however, when the EC:PVA ratio grows, it rises to 75-82%. This is due to increased availability of polymer materials for medication encapsulation. However, the length of the sonication process diminishes trapping efficacy, particularly in the medium-to-high range (10-20 minutes). A shorter sonication duration results in a larger %EE, indicating that an extended sonication period may damage nanoparticles or cause drug leakage. Higher EC:PVA ratios and shorter sonication times yield the highest percentage of EE, while longer sonication and lower EC:PVA ratios result in a significant decrease in %EE. Optimising nanoparticle formulation is essential for therapeutic effects.

#### Independent variables' impact on % of drug release

Figure 8 depicts a 3-D response surface plot that illustrate the influence of the independent variables affect the percentage drug release. Nanosponges benefit from their small size in terms of pharmacodynamics and pharmacokinetics, including release patterns, biodistribution, absorption rate, and cellular uptake. The nanosponges formulations were tested in vitro of release. Drug release characteristics for ethyl cellulose-based formulations.

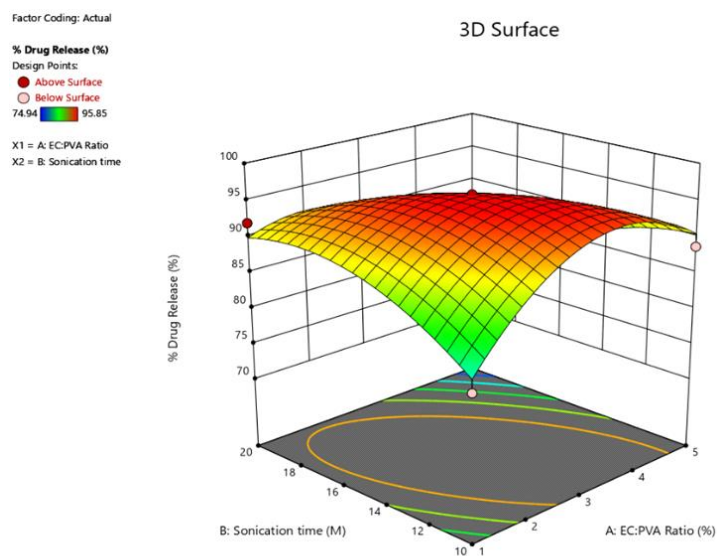


**Fig. 8: Response 3D plots for the effect of EC:PVA ratio (X1) and sonication time (X2) on % drug release**

According to the study, drug release decreases with increasing EC:PVA ratios, going from 90–95% to 75–85%. The study found that as the EC:PVA ratio increases, medication release falls, from 90–95% to 75–85%. The increased EC (polymer) concentration creates a denser matrix. The highest drug release occurs between 12 and 14 minutes into the sonication process and diminishes significantly with increasing or decreasing sonication time. Longer sonication times may cause particle breakage or structural changes, whereas shorter intervals may produce less uniform nanoparticles and faster drug release. The study found that extended sonication times and high EC:PVA ratios promote delayed drug release, while low EC:PVA ratios and moderate sonication times promote rapid drug release. The results show that changing the EC:PVA ratio and sonication period can affect drug release from nanoparticles. A higher EC:PVA ratio and longer sonication time may be beneficial for long-term drug release, whereas a lower EC:PVA ratio and moderate sonication are ideal for fast release.

## 7. EVALUATION OF NANO-SPONGES

### Percentage encapsulation efficiency

The %EE of prepared apremilast nanosponges (NS1-NS9) ranged from 60.22 to 82.75% (Table 2). Based on the results, apremilast nanosponges (NS8) were optimized with % EE (82.75%).

### In-vitro drug release

The *in-vitro* drug release of prepared apremilast nanosponges (NS1–NS9) were found to be in the range of 74.94 – 95.85 % (Table 2). Based on the results, apremilast nanosponges (NS8) were optimized with *in-vitro* drug release (95.85 %).

### Particle size distribution & polydispersity index

The study of Apremilast nanosponges synthesized with ethyl cellulose (CF7) revealed that their average particle size was 213.85 nm, and their polydispersity index (PDI) value was 0.411.

### Zeta potential

Numerous studies have also reported the importance of zeta potential in the interaction between formulation and biological systems. It indicates how stable the developed formulation is and shows the type of charge that is present on the nanosponges' surface. Figure 9 illustrates the corresponding zeta potential of the improved nanosponges formulations, which are -33.3 mv.

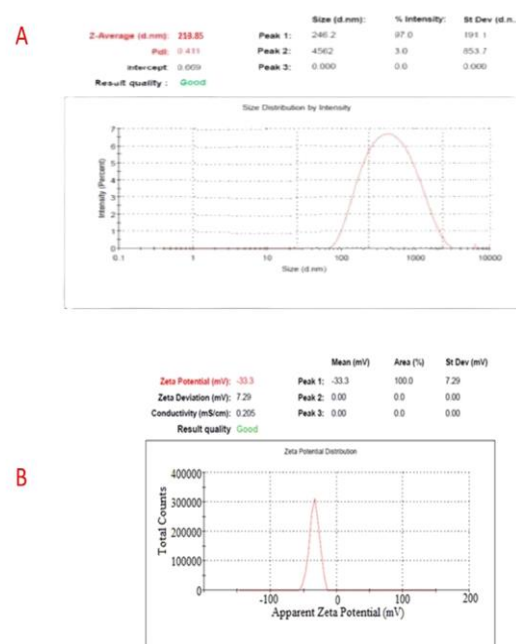


Fig. 9: A. Particle size distribution B. Zeta Potential of optimized batch nanosponges

## Particle Morphology



**Fig. 10: SEM image of Optimized batch of Apremilast Nanosponges**

A spherical shape, a smooth surface with obvious porosity, and uniform particle size are all visible in the SEM image of the Apremilast-loaded nanosponges, shown in fig.10. This allows for uniform release patterns and medication administration. Particle stickiness or drying may result in particle aggregation, affecting stability and dispersibility. Nonetheless, there is no appreciable collapse or deformation, suggesting a stable formulation, and the nanosponges retain their structural integrity. Reducing aggregation is essential to enhancing the topical medication delivery system's effectiveness.

## 8. CONCLUSION

Finally, the study describes the successful development of nanosponges containing apremilast as a cutting-edge topical medicine delivery strategy for wound healing. Pre-formulation studies ensured Apremilast's stability during formulation and compatibility with excipients by providing critical information about its physicochemical properties. The nanosponges created as a result of optimizing important parameters such as the EC:PVA ratio and sonication period had several desirable qualities, including regulated medicine release and small particle size. With a notable drug release profile of 95.85% and a high entrapment efficiency of 82.75%, the optimized nanosponges displayed exceptional stability, showing their potential for improving wound healing therapeutic results.

## ACKNOWLEDGEMENT

"The authors express their gratitude to INSCHEM Lucknow, India, for donating the Apremilast medication sample."

## ETHICAL ISSUES

Not applicable

## CONFLICTS OF INTEREST

The authors certify that they have no competing interests with respect to the data presented in this paper.

## FINANCIAL SUPPORT

"This study received no financial support."

## REFERENCES

- [1] Almadani YH, Vorstenbosch J, Davison PG, Murphy AM. Wound healing: a comprehensive review. In: Seminars in plastic surgery. Thieme Medical Publishers, Inc.; 2021.p. 141–4.
- [2] Nussbaum SR, Carter MJ, Fife CE, DaVanzo J, Haught R, Nussbaum M, et al. An economic evaluation of the impact, cost, and medicare policy implications of chronic nonhealing wounds. Value Heal. 2018;21[1]:27–32.
- [3] Khanam S. A systematic review on wound healing and its promising medicinal plants. IP Int J Compr Adv Pharmacol. 2021;5:170–6.
- [4] Benson HAE, Grice JE, Mohammed Y, Namjoshi S, Roberts MS. Topical and transdermal drug delivery: from simple potions to smart technologies. Curr Drug Deliv. 2019;16[5]:444–60.
- [5] Ravi SC, Krishnakumar K, Nair SK. Nano sponges: A targeted drug delivery system and its applications. GSC Biol Pharm Sci. 2019;7[3]:40–7.
- [6] Tejas J. Patel, Dr. Abdul Mannan Khan DDPS. Formulation and Characterization of Nanosponge Loaded Gel of Apremilast for Topical Delivery. Int J Pharm Res Appl. 2023;08[01]:47–55.

- 
- [7] Priyanka D, Sindhu S, Saba M. Design development and evaluation of ibuprofen loaded nanosponges for topical application. *Int J Chemtech Res.* 2018;11[2]:218–27.
- [8] K. Snehalatha, Roshni Ravindranathan, D. K. Sriram MG. Utility of apremilast in the treatment of psoriasis. *Int J Basic Clin Pharmacol.* 2018;07[08]:1450–3.
- [9] Anwer MK, Mohammad M, Ezzeldin E, Fatima F, Alalaiwe A, Iqbal M. Preparation of sustained release apremilast-loaded PLGA nanoparticles: In vitro characterization and in vivo pharmacokinetic study in rats. *Int J Nanomedicine.* 2019;1587–95.
- [10] Rampado R, Peer D. Design of experiments in the optimization of nanoparticle-based drug delivery systems. *J Control Release.* 2023;358:398–419.
- [11] Reddy CS, Khan KA, Nagaraja CA. Review on the determination of melting point measurement system. *Int J Adv Res Electr Electron Instrum Eng.* 2016;5[2]:975–9.
- [12] Tkachenko Y, Niedzielski P. FTIR as a method for qualitative assessment of solid samples in geochemical research: a review. *Molecules.* 2022;27[24]:8846.
- [13] Patel P, Ahir K, Patel V, Manani L, Patel C. Drug-Excipient compatibility studies: First step for dosage form development. *Pharma Innov.* 2015;4[5, Part A]:14.
- [14] Ali A, Chiang YW, Santos RM. X-ray diffraction techniques for mineral characterization: A review for engineers of the fundamentals, applications, and research directions. *Minerals.* 2022;12[2]:205.
- [15] Horvat M, Mestrovic E, Danilovaski A, Craig D. An investigation into the thermal behaviour of a model drug mixture with amorphous trehalose. *Elsevier.* 2005:1-10.
- [16] Dalu D, Velivela S, Naveentaj S & Giri S. Preparation and evaluation of nanoemulsion formulation by using spontaneous emulsification. *Researchgate.* 2023:837-846.
-